Comparison of seeded region growing and random walk methods for vessel and bone segmentation in CTA images

Ferhat Bozkurt[1], Cemal Köse[2], Ahmet Sarı[3]

[1] Department of Computer Engineering, Faculty of Engineering
Ataturk University, Erzurum, Turkey
fbozkurt@atauni.edu.tr
[2] Department of Computer Engineering, Faculty of Engineering
Karadeniz Technical University, Trabzon, Turkey
ckose@ktu.edu.tr
[3] Department of Radiology, Faculty of Medicine
Karadeniz Technical University, Trabzon, Turkey
asari@ktu.edu.tr

Abstract

Atherosclerosis disease is one of the most important causes of death in the world. Carotid artery stenosis causes narrowing of blood vessels and this forward results with stroke. The carotid arteries enter from the skull cavity and show close proximity to the bone and osteoid structures. Bone tissue and contrast enhanced carotid arteries generally cannot distinguish when vessel evaluation is performed. In this study, the segmentation of carotid arteries and extraction of bone regions are done with seeded region-growing and random walk segmentation methods. And, methods are compared. These methods are applied on different patients' CTA images and the performance evaluations are done with statistical, area and distance based metrics. Region growing and random walk methods in vessel segmentation give approximately similar results. In general, random walk is more successful according to average results in vessel segmentation. It is observed that region growing gives more successful results in bone segmentation and execution time is shorter than random walk method.

1. Introduction

Blood is pumped through the carotid arteries to the head and neck region. Carotid arteries are found as a pair, right and left on both sides of the neck. Carotid arteries are divided into three parts: Common Carotid Artery (CCA), External Carotid Artery (ECA) and Internal Carotid Artery (ICA). Also, Vertebral Arteries (VA) are the vessels on either side of the vertebra that feed the human brain. Carotid arteries consist of vessels extending from the 'Aortic Arch' region to the 'Circle of Willis' region. CCA starts in the aorta and when it reaches neck region, these two vessels are separated as external carotid artery and internal carotid artery. ECA is responsible for pumping blood into areas outside the skull area, as face. Circle of Willis is located in the lower part of the brain. A few arteries come together in this area. In the Willis Circle, ICAs branch to Cerebrum with smaller arteries that supply over %80 oxygen-rich blood [1]. So, these vessels play a major role in the blood supply of the brain to the blood circulation system.

Atherosclerosis disease is one of the most important causes of death in the world. Atherosclerosis is a vascular disease caused by excessive accumulation of fatty material (plaque) and lumen narrowing (stenosis) in the vessel wall. Carotid artery stenosis is narrowing of the artery usually caused by atherosclerosis or bottleneck of the carotid artery lumen. The disease may result in stroke [2, 3]. Contrast-enhanced Computed Tomography Angiography (CTA) is a rapid, inexpensive and minimally invasive method for imaging and measuring carotid plaques [4]. Assessment is made on the image obtained by giving contrast materials to vessel. BTA axial images can be used for grading the severity of the stenosis and for visual examination. Existing CTA techniques allow the expert to perform direct personal assessment and measure the diameter of the carotid lumen and the surrounding soft tissue. Manual carotid lumen segmentation in CTA images is a tedious and time-consuming process that can vary according to the expert observer. The inability to distinguish the vascular-bone structure precisely can lead to misdiagnosis for detection of vascular diseases.

In this study, the segmentation of carotid arteries and extraction of bone regions are done with seeded Region Growing (RG) and Random Walk (RW) segmentation methods and compared. The contrast-enriched vessels can not be separated healthy from the skeletal structure in most parts of the human body. In particular, CTA allows evaluation of the stenosis degree in vascular system, but it requires separation of vessels from calcification and bone structures. The segmentation of vessels in the neck, head and cavity skull region is really difficult process. Removing the obstructed bones and osteoid structures may allow for better evaluation and visualization. So, we both have done the segmentation and extraction of bone structures and segment vessels with seeded RG and RW segmentation methods. And also, two seeded methods are compared according to segmentation accuracy results and execution time. Performance evaluations of methods are done with statistical, area and distance based metrics on different patients' CTA images.

The rest of the paper is organized as follows: Section 2 gives related works about seeded segmentation methods. Section 3 explains the seeded segmentation methods in detail that is used in our study. Section 4 is pointed out the performance metrics and concluded with experimental results.

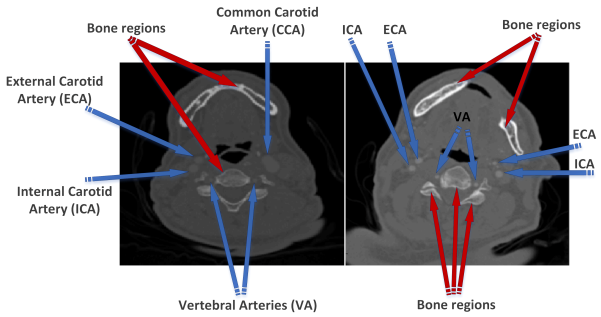

Fig. 1. Arteries and bone regions in CTA images

2. Related work

When previous studies are examined, carotid artery segmentation is performed from the images obtained by ultrasonography and angiography methods [5, 6]. Lumen measurement at each layer of CTA is more suitable for determining stenosis value. The most difficult step in image analysis is image segmentation according to related works. Segmentations can be achieved (semi)automatically or manually.

Seeded region growing (SRG) has become popular in recent years due to its rapid convergence, accuracy and incentive features. This method introduced by Adams and Bischof [7], and it is fast, robust and immune to parameter settings. Fan et al. [8], was done an extensive and comparative study about SRG. They presented about the automatic SRG algorithm and automatic seed selection. Several variants of SRG have been proposed for medical image segmentation, for example adaptive region growing algorithm that was presented by Wu et al. [9]. Rai and Nair [10], proposed a gradient based SRG method that control the region grow operation by using a gradient based homogeneity criteria.

Random walk method was proposed by Grady [12]. And it's a semi-automatic and interactive segmentation. Since it is an interactive method, it is requested to determine the seed point as starting point from user. The random walk ensures unique and quality solution which is resistant to weak object boundaries. M'hiri et al. [13] used random walk for coronary arteries segmentation. The vesselness information was integrated to random walker formulation with their method. Li et al. [14] used random walk for retinal blood vessel segmentation.

3. Seeded segmentation methods

We present two methods for segmenting carotid arteries and bone: region growing and random walk segmentation. These techniques are seeded segmentation algorithms; they begin with a point, called the seed point, which is defined to be within vessel or bone intensity level. Carotid artery region is segmented from starting one or more starting same seed points for RG or RW techniques. Similarly, bone region is segmented by using RG or RW techniques. Same starting seeds points are taken from bone intensity interval for RG or RW techniques. In CTA images, we can select the seeds manually signed points or automatically from vessel or bone intensity level interval. Thus, we can analyze and compare the segmentation results that are achieved from RG and RW methods for same region. RG and RW methods, some advantages and disadvantages are mentioned for carotid artery and bone segmentation in this section.

3.1. Region growing method

The base point in the region-based methods is to divide the pixels in similar intensity with regions according to the given homogeneity value. For adjacent regions, region growing is a suitable segmentation method and is almost an unsupervised method. The region growing method is based on the selection of a seed pixel and the neighboring pixels with similar statistical values come together to become a region. It uses standard deviation and average intensity to grow the area [7]. The most commonly used procedure of changing the seed points in region growing method is (1). Herein, the selected seed is compared to its neighbors to check whether it has the same uniform distribution under a certain $\triangle$ error. In this method, a pixel that differs by $\triangle$ threshold value is added to the new region, and new region average is calculated with the added pixel in the region. The next comparison is done according to the μ_R average of newly found region.

$$Img(i,j)\_seg = \begin{cases} Bone, & if\ |Img\_org(i,j) - \mu_R| \leq \triangle \\ Not\ bone, & \text{Otherwise} \end{cases} \quad (1)$$

Herein; Img(i,j)_seg represents the segmentation result, Img_org(i,j) represents the intensity level of the current pixel, μ_R represents the average of the currently segmented pixels, and $\triangle$ reference threshold value.

The seeds are identified experimentally by examining the local histograms. The interval between highest intensity level of the vessel and maximum intensity level in the image is taken for bone segmentation. For example, bone segmentation between the point where the vessel ends and the upper limit [1500,4096] was taken as the seed interval. When doing vessel segmentation, the vessel segmentation is performed by excluding the previously segmented bone region, and seeds within the interval that are selected between [1150-4096].

If connectivity in the vessel region is not taken into consideration, you can not separate the vessel-bone region only with intensity-based thresholding alone. Two adjacent features are considered as pixel connected, therefore they are considered to belong to the same region. There are two possible definitions of connectivity; 4-connectivity; and 8-connectivity [15]. 8-connectivity is preferred to explore pixel similarity with more neighbors of the pixel. Eight neighboring pixels of each seed point are examined. Each neighboring pixel providing the threshold criteria is added to the feature set. And this added pixel becomes a new seed point. Region growing requires a threshold criterion and one or more seed points [16]. Threshold value is obtained from the inter-pixel intensity differences in the regions according to the homogeneity criterion by studying the feature space in the vessel and bone regions. The variance of a region is related to the heterogeneity pixels in the region. When the pixels are homogeneously distributed, the value of the variance is close to zero. On the other hand, variance has a big value in blocks with very diverse pixel intensities. So, it can be found in the low intensity level in the bone due to the spongy structure as well as the very high intensities in the bone. We get threshold value high for example $\triangle$=100 while doing bone segmentation, but since the vessel region is more homogeneous when we are doing vessel segmentation, we get the threshold value $\triangle$ = 9 because the neighboring pixel values are very close to each other. These values were determined experimentally. The segmentation of the bone region which is a relatively problematic area for vascular segmentation, is could

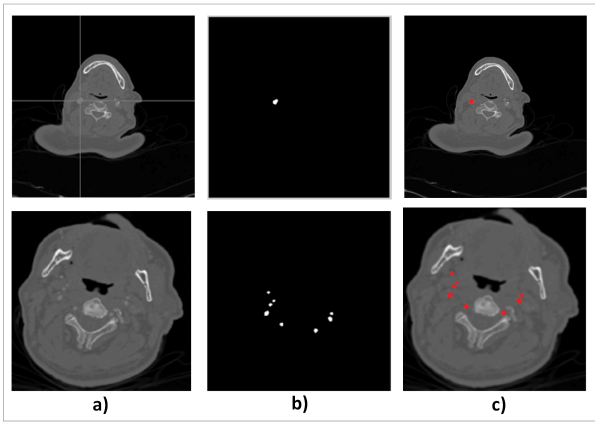

Fig. 2. Region growing segmentation in CTA image

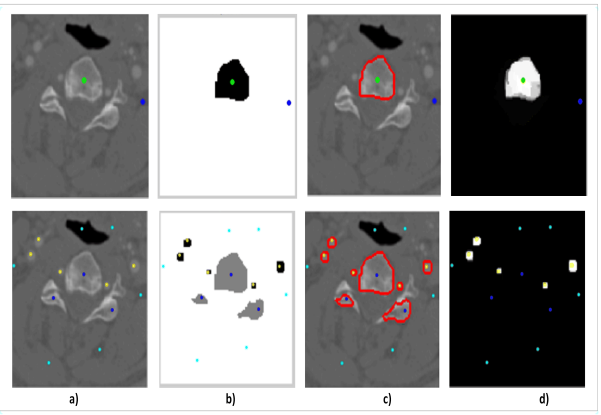

Fig. 3. Random walk segmentation in CTA image

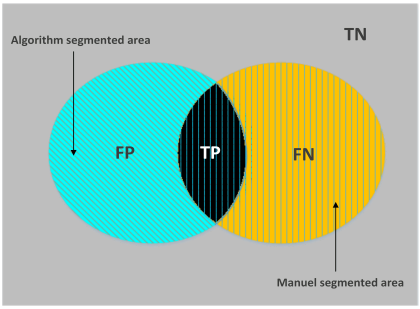

Fig. 4. The used areas to measure segmentation accuracy

done by taking the high intensity value interval in bone tissue as seeds. However, vessel segmentation with region growing is confused with the vertebral bone and parts of the scull in places where the vessel regions are very close to the bone.

3.2. Random walk method

In this method, the image is modeled as graph. The nodes represent the pixels in the image and pixels are linked to the other nodes by the weighted edges according to the similarity to the neighboring pixels. The interactive image segmentation method requires from the user to indicate seed points as starting points. These seed points are usually divided into two classes as the background and the foreground, and seed points which belong to more classes can also be indicated. For this method, seeds are selected from the experimentally determined interval as region growing method. User defined seed points are called as labelled pixels. The other pixels in the image are called as unlabeled pixels and an imaginary random walker continue to process from these unlabeled pixels. This walker moves to the other pixels depending on the edge weight. The probability of the first arrival to these pixels is calculated along the random walk for all labelled pixels. The first labelled seed which has the highest probability of random walk leaving from an unlabeled pixel, is labeled with the same label value according to the calculated probabilities. According to this method, after all the unlabeled pixels are labeled, image is segmented into partitions. This method was first introduced by Leo Grady in [11] as a conference and later as a journal [12].

$$\omega_{ij} = \exp(-\beta(g_i - g_j)^2) \tag{2}$$

Different features from pixels can be used to create weighted graphs. g_i and g_j intensity values are used to calculate the weight of the ω_{ij} that connects neighboring pixels in (2). Nodes, edges and weights can be used to construct the laplace matrix L to be used in the calculation of the probabilities.

$$Q(x) = x^T Lx = \sum_{e_{ij}} w_{ij}(x_i - x_j)^2 \tag{3}$$

Nodes represent the v_i and v_j pixels. The e_{ij} is the edge between the nodes and x_i and x_j are the variables representing the original values associated with the nodes. Each random walker is released from the node and optimizes the (3) energy formula.

When seed points are labeled F as foreground and B as background, it is $v_i \in F$ for $x_i = 1$ and $v_i \in B$ for $x_i = 0$. When all labeled nodes in the image are denoted by $S = F \cup B$ and unlabeled nodes are denoted by $\bar{S}$, the optimal energy minimization problem can be solved with (4).

$$L_{\bar{S},\bar{S}}{}^{x}{}_{\bar{s}} = -L_{\bar{S},S^{x}{}_{s}} \tag{4}$$

When associating the original values that represent and calculate the similarity to the labels for the nodes with the L matrix, minimization problem take the form of the (6) for F and B positive diagonal matrices.

$$Q(x) = x^T L_x + \gamma((1-x)^T F(1-x) + x^T Bx) \tag{5}$$

$$= \sum_{e_{ij}} w_{ij}(x_i - x_j)^2 + \gamma(\sum_{v_i} f_{ij}(1-x_i)^2 + \sum_{v_i} b_i {x_i}^2) \tag{6}$$

When the probabilities are to be associated with a color model, the similarities to the labeled nodes that are seed points will represent the closeness of the f_i ve b_i values to the respective colors.

Region growing and random walk segmentations were done with one or more seed points as shown in Fig. 2 and Fig. 3.

4. Experimental results

In this study, carotid artery and bone segmentation is performed by using RG and RW methods on CTA data which is obtained from Department of Radiology, Karadeniz Technical University, Farabi Hospital. Scanned CTAs have a large number of two-dimensional layer images of different patients. Each CTA data consists of approximately 350-400 layer images in DICOM format and 12-bit grayscale images with size of 512x512 pixels. The segmentations were implemented in MATLAB R2012a and executed on 2.40 GHZ Intel Core i7 Notebook with 16GB RAM.

The statistical, area and distance-based metrics were used to evaluate the accuracy of the segmentation. The validity of the segmentation methods are done by comparing the areas of the segmented vessels that correspond to the areas indicated by the expert clinician. For example, vessel regions are manually marked by radiologist experts on an original CTA images as shown in Figure.5 with green borders. In other words, green borders represent the vessel lumens or borders in CTA images according to expert opinion. Manual segmentations are done by experts from a few slices images that contains related carotid artery regions with our own MATLAB dicom viewer software. Statistical and area-based metrics comparisons are made between the results of segmented with RG/RW methods and the regions which are determined by the expert clinician. In order to perform these measurements, we firstly defined the areas that are used to compare the accuracy of the segmentation as shown in Fig. 4. TP is the number of true positive pixels, this means that the number of pixels with algorithm segmentation results match with manual segmentation. FP is the number of false positive pixels, this means that the number of pixels that the automatic segmentation has segmented but manual segmentation is not. TN is exactly the number of incorrect pixels, this means that the number of pixels which the automatic and manual segmentation do not match. FN is the number of erroneous negative pixels, this means that manual segmentation marks area for segmentation but that the algorithm does not segment it. The following statistical and area-based performance metrics were derived by using these definitions.

Sensitivity (SE), Specificity (SP), Precision (PR) and Accuracy (ACC) are described in terms of TP, TN, FN and FP [17, 18]. These statistical metrics are used for accuracy evaluation.

We also used area-based performance metrics that are described in terms of TP, TN, FN and FP. The AO (Area Overlap) measures the proportional area that is correctly defined by the algorithm. The Area Difference (AD) measures the proportional area that is detected incorrectly by the algorithm. Dice Smilarity (DS) is the measure of similarity between two segmented areas [19, 20]. We used this metric to measure the level of agreement between two data: manual and algorithm segmented area.

$$AO = \frac{TP}{TP + FN + FP} \times 100\% \tag{7}$$

$$AD = \frac{FP + FN}{TP + FN + FP} \times 100\% \tag{8}$$

$$DS = 2\,x\,(TP)/\left((TP + FN) + (FP + TP)\right) \tag{9}$$

We used distance-based metric to evaluate the vessel lumen and outer wall boundaries. For computing the distance-based metrics, two contours were first matched on a point by-point. We measured distances of two contours on a point-by-point. Distance between each pair of points on the two contours was computed that contour (A) segmented by the algorithm as $\{a_i : i = 1...K\}$ and the vertices of the manually segmented contour (M) as $\{m_n : n = 1...N\}$. Three distance-based metrics were computed, which are mean absolute difference (MAD), root-mean-squared-error of distance (RMSE) and Hausdorff distance (MAXD) [20].

$$d(a_i, M) = \min_n \|a_i - m_n\| \tag{10}$$

$$MAD = \frac{1}{K}\sum_{i=1}^{K} d(a_i, M) \tag{11}$$

$$RMSE = \sqrt{\frac{1}{K}\sum_{i=1}^{K} d(a_i, M)^2} \tag{12}$$

$$MAXD = \max_{i\in[1,K]} \{d(a_i, M)\} \tag{13}$$

The performance evaluation of RG/RW methods on CTA images were done according to these performance metrics. For instance, vessel segmentation results are compared by using RG/RW methods with same seed points on CTA images as shown in Fig. 5. The segmentation results and ground truth images of carotid arteries are compared with each other. In other

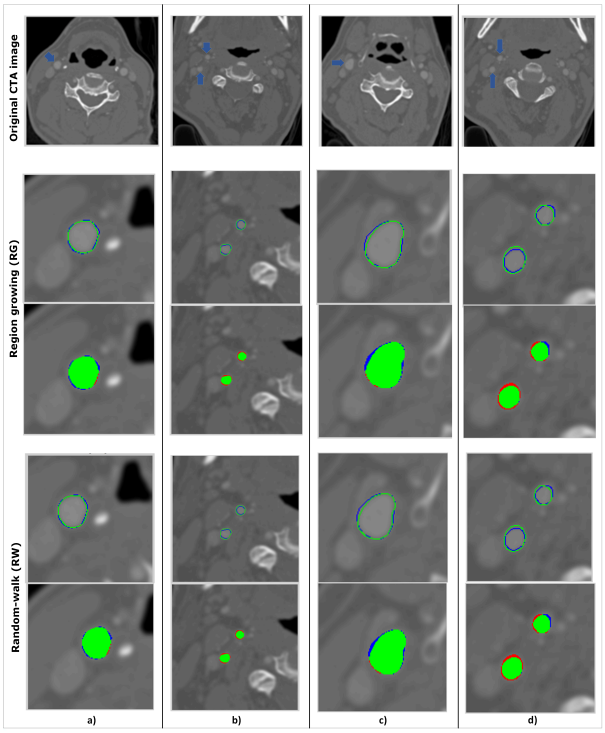

Fig. 5. Comparing RG and RW vessel segmentation at same seed points on four different CTA image. (a) for CTA Img.1, (b) for CTA Img.2, (c) for CTA Img.3, (d) for CTA Img.4 and results in Table 1. The second-fourth rows show the vessel edges show green:manuel segmentation, blue:automatic segmentation. The third-fith rows show the vessels full marked means that green:overlapped(true), blue:over, red:under segmentation.

Table 1. Comparision of RG/RW vessel segmentation at same seed points on four different CTA images as shown in Fig. 5.

Image	Method	Statistical results				Area-based results			Distance-based results		
		SE	SP	ACC	PR	AO (%)	AD (%)	DS (%)	MAD (mm)	RMSE (mm)	MAXD (mm)
CTA Img.1	RG	0.9895	0.9998	0.9998	0.9341	92.49	7.51	96.10	0.05	0.29	2.45
	RW	0.9895	0.9998	0.9998	0.9470	93.76	6.24	96.78	0.05	0.28	2.24
CTA Img.2	RG	0.7982	0.9999	0.9995	0.9999	81.04	20.18	88.78	0.10	0.39	2.45
	RW	0.8104	0.9999	0.9995	0.9999	79.82	18.96	89.53	0.09	0.39	2.45
CTA Img.3	RG	0.9927	0.9997	0.9996	0.9310	92.46	7.54	96.08	0.07	0.33	2.00
	RW	0.9903	0.9997	0.9996	0.9344	92.59	7.41	96.15	0.08	0.35	2.00
CTA Img.4	RG	0.8182	0.9999	0.9994	0.9581	78.99	21.01	88.26	0.12	0.42	2.24
	RW	0.8209	0.9999	0.9994	0.9582	79.26	20.74	88.43	0.12	0.41	2.24

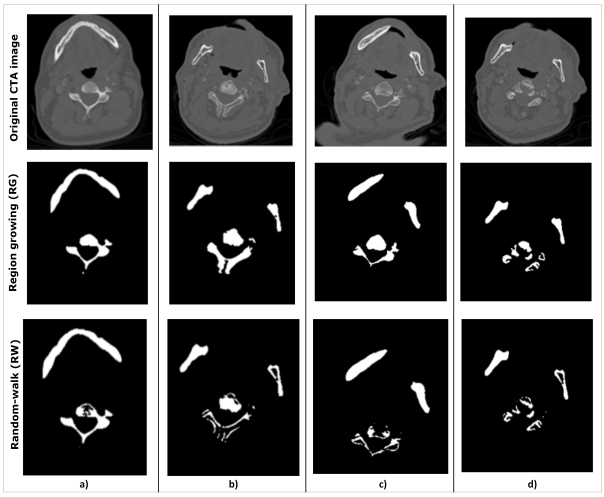

Fig. 6. Comparing RG and RW bone segmentation at same seed points on four different CTA images.

words, experts are marked the vessels manually on our DICOM viewer software, then RG/RW segmentation results are overlapped with manual segmentations. In Fig. 5, green drawing shows the manual segmentation blue shows RG/RW segmentation results. And also, vessels are full marked with green means that overlapped (true), blue means that over segmentation, red means that under segmentation. According to Table 1 performance results; both methods give similar results for the same images and seed points, but it is seen that the DS result obtained with RW method is higher than RG method's result.

Bone segmentation results are compared by using RG/RW methods with same seed points on CTA images as shown in Fig. 6. According to experts' evaluations, RG method is more successful than RW methods at bone segmentation. Because, RG included more regions that have low intensity as spongiform tissue than RW method. As shown in Fig. 6, RG is especially successful in spongiform structures and include more regions than RW.

The performance evaluation of RG/RW methods was also done on 56 CTA images. This data was taken randomly from 10 different patients' CTA data set and from different slices in a CTA data. Beforehand, all of the carotid artery points are marked in expert control. Then, vessel segmentation was done with RG/RW methods on this dataset. As pointed in Table 2, five images were taken from CTA-1 dataset and segmented. Seven images were taken from CTA-2 dataset and segmented, and so on. In table 2 the statistical, area and distance based measure scores are shown, which were obtained by RG method for vessel segmentation on 56 CTA data set. According to this table, average %89 Dice similarity %99 accuracy values were obtained. Similiarly, vessel segmentation was done on same CTA images by using RW method. In table 3 the statistical, area and distance based measure scores are shown, which were obtained by RW method for vessel segmentation on 56 CTA data set. According to this table, approximately average %90 Dice similarity %99 accuracy values were obtained.

RG is faster than RW method in segmentation for each slice to segment vessel and bone regions. Vessel segmentation by using RG method takes 0,4 seconds mean computation time for each slice. Vessel segmentation by using RW method takes 0,6 seconds mean computation time for each slice And, vessel segmentation for all dataset takes approximately 25 seconds by using RG method and 34 seconds by using RW method. Similarly, bone segmentation by using RW method takes long time than RG method. Bone segmentation for all dataset takes approximately 105 seconds by using RG method and 122 seconds by using RW method.

5. Conclusion

Bone tissue and contrast enhanced carotid arteries generally cannot distinguish when vessel evaluation is performed. The segmentation of carotid arteries and extraction of bone regions were done with seeded region-growing and random walk segmentation methods. Two methods were applied on different patients' CTA images and the performance evaluations were done and compared with each other. We used performance metrics to measure agreement level of two data: manual and algorithm segmented area. The segmentation results and ground truth images of carotid arteries were compared with each other. Performance evaluations of methods were done with statistical, area and distance based metrics on different patients' CTA images.

RG and RW methods in vessel segmentation give approximately similar results. In general, RW is more successful according to average results in vessel segmentation. RG method is more successful than RW methods at bone segmentation. It is observed that RG gives more successful results in bone segmentation and execution time is shorter than RW method. Because, RG included more regions that have low intensity as spongiform tissue than RW method. The performance evaluation of RG/RW methods were done on 56 CTA images. By using RG method, average %89 Dice similarity %99 accuracy

Table 2. The performance evaluation of region growing segmentation on 56 CTA images

CT data set	# of seg. image	Statistical results				Area-based results			Distance-based results		
		SE	SP	ACC	PR	AO (%)	AD (%)	DS (%)	MAD (mm)	RMSE (mm)	MAXD (mm)
1	5	0.7875	0.9998	0.9994	0.9999	85.76	14.24	88.56	0.11	0.35	2.18
2	7	0.8512	0.9998	0.9994	0.9492	80.66	19.34	88.13	0.13	0.43	2.26
3	6	0.9518	0.9996	0.9996	0.9397	88.92	11.08	87.15	0.15	0.38	2.32
4	4	0.9811	0.9998	0.9997	0.9382	92.75	7.25	92.32	0.07	0.29	1.96
5	5	0.7891	0.9997	0.9995	0.9413	90.25	9.75	89.32	0.09	0.31	2.18
6	6	0.8347	0.9999	0.9994	0.9582	78.48	21.52	88.24	0.13	0.42	2.26
7	8	0.7917	0.9999	0.9996	0.9512	83.78	16.22	89.49	0.10	0.33	2.20
8	6	0.9815	0.9998	0.9997	0.9346	91.88	8.12	90.17	0.15	0.40	2.27
9	5	0.9515	0.9997	0.9995	0.9428	78.87	21.13	87.47	0.14	0.39	2.29
10	4	0.9785	0.9995	0.9994	0.9512	89.85	10.15	89.58	0.12	0.41	2.23

Table 3. The performance evaluation of random walk segmentation on 56 CTA images

CT data set	# of seg. image	Statistical results				Area-based results			Distance-based results		
		SE	SP	ACC	PR	AO (%)	AD (%)	DS (%)	MAD (mm)	RMSE (mm)	MAXD (mm)
1	5	0.7928	0.9998	0.9995	0.9998	86.39	13.61	89.26	0.10	0.30	2.10
2	7	0.8672	0.9998	0.9994	0.9491	81.99	1.01	88.96	0.12	0.41	2.21
3	6	0.9676	0.9996	0.9996	0.9488	89.25	10.75	88.26	0.14	0.35	2.26
4	4	0.9862	0.9998	0.9997	0.9391	93.59	6.41	93.10	0.06	0.27	1.90
5	5	0.7982	0.9997	0.9995	0.9495	91.17	8.83	90.11	0.08	0.29	2.11
6	6	0.8472	0.9999	0.9994	0.9591	79.17	20.83	88.98	0.12	0.41	2.24
7	8	0.8169	0.9999	0.9996	0.9591	84.89	15.11	90.22	0.09	0.29	2.13
8	6	0.9854	0.9998	0.9997	0.9425	92.25	7.75	90.34	0.14	0.37	2.21
9	5	0.9779	0.9997	0.9995	0.9568	80.33	19.67	88.69	0.13	0.34	2.22
10	4	0.9892	0.9995	0.9994	0.9611	90.59	9.41	90.11	0.10	0.38	2.15

values were obtained. By using RW method approximately average %90 Dice similarity %99 accuracy values were obtained. RG is faster than RW method in segmentation for each slice to segment vessel and bone regions. Bone segmentation by using RW method takes long time than RG method. Also, vessel segmentation only with region growing or random walk confused with the vertebral bone and parts of the scull in places where the vessel regions are very close to the bone.

6. References

[1] B. J. Alpers, R. G Berry, R. M. Paddison, "Anatomical studies of the circle of Willis in normal brain", *AMA Archives of Neurology & Psychiatry,* 81(4), 409-418, 1959.

[2] H. R. Hemmati, A. R. Kamali-asl, A. R. Talebpour, M. Alizadeh, and S. Shirani, "Segmentation of carotid arteries in computed tomography angiography images using fast marching and graph cut methods", *In Electrical Engineering (ICEE), 2013 21st Iranian Conference,* pp. 1-5, IEEE, 2013.

[3] J. Frostegård, "SLE, atherosclerosis and cardiovascular disease.", *Journal of internal medicine*, 257(6), 485-495. 2005.

[4] D. Green, and D. Parker, "CTA and MRA: visualization without catheterization.", *In Seminars in Ultrasound, CT and MRI*, Vol. 24, No. 4, pp. 185-191, WB Saunders, 2003.

[5] A. Hedblom, "Blood vessel segmentation for neck and head computed tomography angiography.", 2013.

[6] P. Mattsson and A. Eriksson, "Segmentation of carotid arteries from 3D and 4D ultrasound images.", 2002.

[7] R. Adams and L. Bischof, "Seeded region growing", *IEEE Transactions on pattern analysis and machine intelligence*, 16(6), 641-647, 1994.

[8] J.Fan, G.Zeng, M. Body and M. S. Hacid, "Seeded region growing: an extensive and comparative study", *Pattern recognition letters*, 26(8), 1139-1156, 2005.

[9] J. Wu, F. Ye, J. Ma, X. Sun, J. Xu, and Z. Cui, "The segmentation and visualization of human organs based on adaptive region growing method",*In Proc. Int. Conf. Comp. Inf. Tech.*, pp. 439-443, 2008.

[10] H. Rai, and T. R. Nair, "Gradient Based Seeded Region Grow method for CT Angiographic Image Segmentation", *Inter JRI Computer Science and Networking*, vol. 1, no.1, pp. 1-6, July 2009.

[11] L. Grady, G.Funka-Lea, "Multi-Label Image Segmentation for Medical Applications Based on GraphTheoretic Electrical Potentials", *Proc. of the 8th ECCV Workshop on Computer Vision Approaches to Medical Image Analysis and Mathematical Methods in Biomedical Image Analysis*, pp. 230-245, 2004.

[12] L. Grady, "Random Walks for Image Segmentation", *IEEE Trans. on Pattern Analysis and Machine Intelligence*, Vol. 28, No. 11, pp. 1768-1783, Nov., 2006.

[13] F. M'hiri, L. Duong, C. Desrosiers and M. Cheriet, "Vesselwalker: Coronary arteries segmentation using random walks and hessian-based vesselness filter", *In Biomedical Imaging (ISBI), 2013 IEEE 10th International Symposium*, pp. 918-921, 2013.

[14] Y. Li, H. Gong, W. Wu, G. Liu and G. Chen, "An automated method using hessian matrix and random walks for retinal blood vessel segmentation," *2015 8th International Congress on Image and Signal Processing (CISP)*, Shenyang, pp. 423-427, 2015.

[15] N. Efford, "Digital image processing: a practical introduction using java", *Addison-Wesley Longman Publishing*, ISBN 0-201 -59623-7, 2000.

[16] Y.T. Wu, F.Y. Shih, J. Shi and Y. T. Wu, "A top-down region dividing approach for image segmentation", *Pattern recognition*, 41(6), 1948-1960, 2008.

[17] M. Hassan, A. Chaudhry, A. Khan and J. Y. Kim, "Carotid artery image segmentation using modified spatial fuzzy c-means and ensemble clustering.", *Computer methods and programs in biomedicine*, 108(3), pp. 1261-1276, 2012.

[18] K. Bowyer, "Validation of Medical Image Analysis Techniques", in M. Sonka et al. (Eds.), "Handbook of Medical Imaging", vol. 2, *SPIE Press*, 2000, chapter 10, pp.571-575.

[19] A. M. Santos, J. M. R. Tavares, L. Sousa, R. Santos, P. Castro and E. Azevedo, "Automatic segmentation of the lumen of the carotid artery in ultrasound B-mode images.", *In SPIE Medical Imaging (pp. 86703I-86703I). International Society for Optics and Photonics*, 2013.

[20] M. Zouqi, and J. Samarabandu, "2D ultrasound image segmentation using graph cuts and local image features.", *In Computational Intelligence for Image Processing, 2009. CIIP'09. IEEE Symposium* pp. 33-40, IEEE, 2009.